CLIMATOLOGY

Organic carbon burial is paced by a ~173-ka obliquity cycle in the middle to high latitudes

He Huang[1,2], Yuan Gao[1,2]*, Chao Ma[3], Matthew M. Jones[4], Christian Zeeden[5], Daniel E. Ibarra[6,7], Huaichun Wu[1,8], Chengshan Wang[1,2]*

Earth's climate system is complex and inherently nonlinear, which can induce some extraneous cycles in paleoclimatic proxies at orbital time scales. The paleoenvironmental consequences of these extraneous cycles are debated owing to their complex origin. Here, we compile high-resolution datasets of total organic carbon (TOC) and stable carbon isotope ($\delta^{13}C_{org}$) datasets to investigate organic carbon burial processes in middle to high latitudes. Our results document a robust cyclicity of ~173 thousand years (ka) in both TOC and $\delta^{13}C_{org}$. The ~173-ka obliquity–related forcing signal was amplified by internal climate feedbacks of the carbon cycle under different geographic and climate conditions, which control a series of sensitive climatic processes. In addition, our new and compiled records from multiple proxies confirm the presence of the obliquity amplitude modulation (AM) cycle during the Mesozoic and Cenozoic and indicate the usefulness of the ~173-ka cycle as geochronometer and for paleoclimatic interpretation.

INTRODUCTION

The Milankovitch theory provides a remarkable tool to investigate climatic response to latitudinally varying top-of-atmosphere insolation changes at ten thousand– to million-year time scales (*1*, *2*). Despite conventional Milankovitch cycles [i.e., ~100 and ~405 thousand years (ka) for eccentricity, ~40 ka for obliquity, and ~19 and 23 ka for precession] being well documented in geological archives, numerical integration of orbital parameters indicates the existence of longer cycles, which are mainly manifested as amplitude modulation (AM) of shorter cycles (*2*, *3*). These AM cycles often lead to a nonlinear process between the external (orbital) forcing and internal Earth system climate feedbacks and play a key role in pacing climatic changes, species evolution, and global carbon cycle (*4*–*6*). The orbital forcing of nonlinear features in this study is inspired by the third criterion in (*7*), which claims that the spectral results of a nonlinear system respond to periodic orbital forcing and exhibit frequencies not present in the original driven forcing (*7*, *8*).

Numerous studies have focused on the 2.4-million-year (Ma) eccentricity period and the 1.2-Ma obliquity AM periods, which originate from gravitational interactions between Earth and Mars (*1*, *4*, *9*–*12*). While the presence of a ~173-ka cycle is established from astronomical solutions [e.g., (*2*)], recently, it was prominently detected in the sedimentary and geochemical proxies of the Middle Eocene and Late Cretaceous as a result of AM of the ~40-ka obliquity cycle (*13*–*15*). This obliquity AM cycle has been used as a new geochronometer to construct the geological time scale for closing the "Middle Eocene time scale gap" (*14*) and to refine the duration of Cretaceous Oceanic Anoxic Event 2 (OAE2) (*13*). The global carbon cycle, with many climatic feedbacks, responds to this astronomical forcing through changes in hydrological processes and preservation conditions of sedimentary basins (*16*), although few datasets have been presented to confirm changes in the global carbon cycle and climate related to the ~173-ka obliquity AM cycle.

Organic carbon (OC) burial is a key component of Earth's carbon cycle, representing a major sink of CO_2 from the ocean-atmosphere carbon reservoirs (*15*). Milankovitch cycles have been widely detected in TOC content time series, highlighting the influence of precession and/or eccentricity cycles at low latitudes controlled by seasonal insolation intensity (*17*, *18*). The linear and nonlinear obliquity effect on TOC and therefore the carbon cycle is less understood but seems to be more prominent in middle to high latitudes linked to the insolation latitudinal distribution and low-latitude teleconnections (*15*).

Here, we present analyses of multiple high-resolution TOC and stable organic carbon isotope ($\delta^{13}C_{org}$) records from the middle to high latitudes during the past 100 Ma (Fig. 1) and evaluate the effect of obliquity on OC burial, especially in the temporal expression of the ~173-ka orbital cycle. These records include a new TOC and $\delta^{13}C_{org}$ record from the Late Cretaceous Songliao Basin, two published TOC records from the Miocene Tarim Basin and Pleistocene Lake El'gygytgyn, and two published $\delta^{13}C_{org}$ records from the Western Interior Basin and Bohemian Cretaceous Basin (Fig. 1). All records indicate notable linear (i.e., directly respond to ~40-ka obliquity) and nonlinear (i.e., identified by the obliquity AM or clipped/rectified obliquity signal) responses in OC burial to obliquity and its AM cycles (Figs. 2 and 3). Furthermore, we compile published records discussing ~160- to 200-ka cycles, which were interpreted to represent the ~173-ka obliquity cycle, from multiple paleoclimatic proxies throughout the past 200 Ma (table S1). We infer that the ~173-ka cycle is a considerable factor on modulating the global carbon cycle and climate at orbital scale through nonlinear climatic effects.

[1]State Key Laboratory of Biogeology and Environmental Geology, China University of Geosciences (Beijing), Beijing 100083, China. [2]School of Earth Sciences and Resources, China University of Geosciences (Beijing), Beijing 100083, China. [3]State Key Laboratory of Oil and Gas Reservoir Geology and Exploitation and Institute of Sedimentary Geology, Chengdu University of Technology, Chengdu 610059, China. [4]Department of Earth and Environmental Sciences, University of Michigan, Ann Arbor, MI 48109, USA. [5]Leibniz Institute for Applied Geophysics, Stilleweg 2, 30655 Hannover, Germany. [6]Department of Earth and Planetary Science, University of California, Berkeley, Berkeley, CA 94720, USA. [7]Institute at Brown for Environment and Society and Department of Earth, Environmental and Planetary Sciences, Brown University, Providence, RI 02912, USA. [8]School of Ocean Sciences, China University of Geosciences (Beijing), Beijing 100083, China.
*Corresponding author. Email: yuangao@cugb.edu.cn (Y.G.); chshwang@cugb.edu.cn (C.W.)

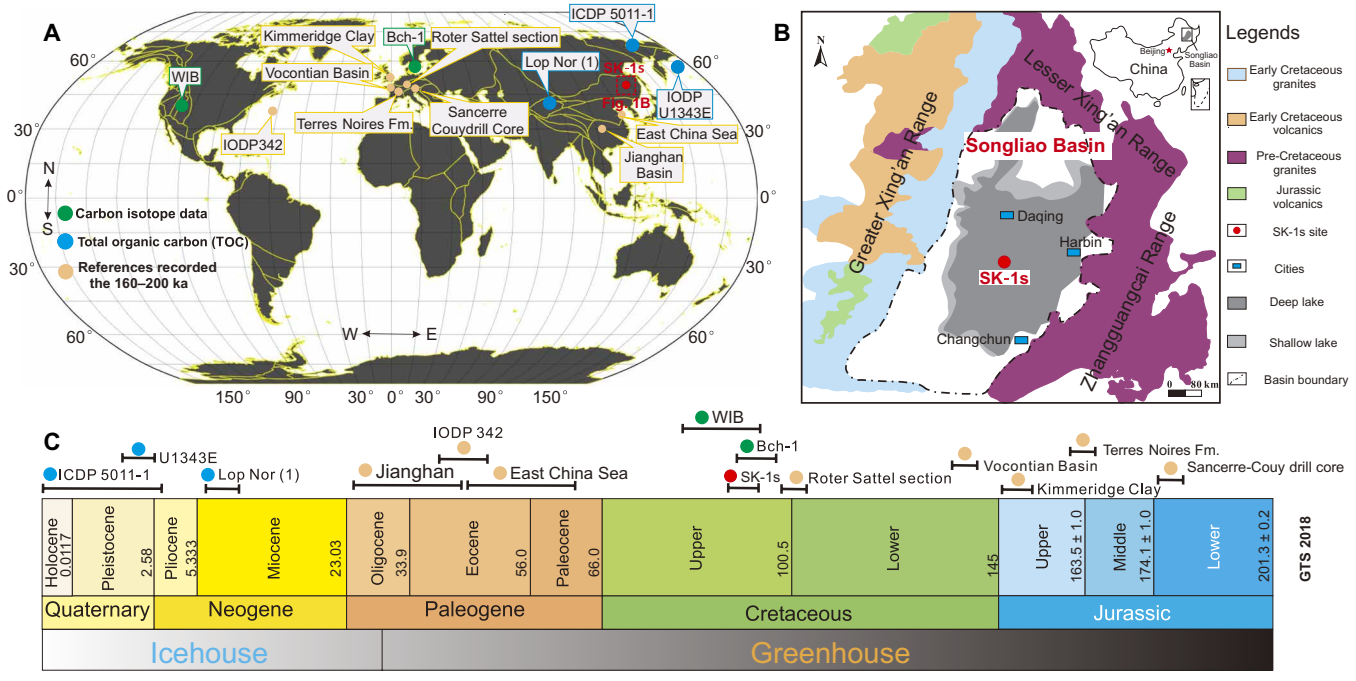

Fig. 1. Geographical and temporal compilation of sedimentary records of ~160- to 200-ka cycles (interpreted as ~173-ka obliquity cycle) throughout the past 200 Ma. (**A**) Geographical distribution of study sites related in this study in a modern global map (created from http://portal.gplates.org/map/). Green circles represent compiled OC isotope data during the Late Cretaceous; WIB, Western Interior Basin (*49*); Bch-1, Bohemian Cretaceous Basin (*50*). Blue circles represent the collected TOC data, ICDP 5011-1 (*25*), U1343E (*59*), and Lop Nor (1) (*24*). Orange circles represent the references recording the ~160- to 200-ka signals possibly linked to the s_3-s_6 obliquity AM cycle, Jianghan Basin (*60*), IODP 342 (*14*), East China Sea Shelf Basin (*4*), Roter Sattel section (*13*), Vocontian Basin (*61*), Kimmeridge Clay (*18*), Terres Noires Fm. (*62*), and Sancerre-Couy drill core (*63*). (**B**) Schematic map of Songliao Basin and the location of the SK-1s drilling core. (**C**) Geological age distribution of the study sites in this study, GTS 2018 (URL: http://stratigraphy.org/ICSchart/ChronostratChart2018-08.pdf) (*64*). Additional data are displayed in table S1.

RESULTS

Study sites and data compilation

In this study, we generate new high-resolution TOC and $\delta^{13}C_{org}$ chemostratigraphic data from the Late Cretaceous Songliao Basin and compile several available high-resolution TOC curves from middle to high paleolatitudes spanning the past 100 Ma (Fig. 1). In addition, we have compiled the published cyclostratigraphic literature related to the ~160- to 200-ka cycles recorded in multiple climatic proxies spanning the past 200 Ma and listed their possible signal interpretation (Fig. 1 and table S1). In the main text, we focus on the analysis of three TOC records and two $\delta^{13}C_{org}$ records.

Late Cretaceous Songliao Basin and SK-1s core (northeast China)

The Songliao Basin in northeast China was a large paleo-lake basin at mid-latitude East Asia in the Late Cretaceous (~40°N to 50°N; Fig. 1). The Qingshankou Formation is a unit of gray to black mudstones deposited in a deep lacustrine environment (Fig. 1B). The studied interval in the SK-1s scientific core spans the middle Turonian and early Coniacian of the Late Cretaceous (91.9 to 89.5 Ma). Its age model is well constrained by biostratigraphy, magnetostratigraphy, cyclostratigraphy, $\delta^{13}C_{org}$ chemostratigraphy, and U-Pb radioisotope geochronology (*19*–*23*). A total of 203 samples were collected from the Qingshankou Formation for TOC and $\delta^{13}C_{org}$ measurements (table S2).

Late Miocene Tarim Basin (west China)

The Lop Nor (1) core (~40°N) is located in the eastern part of the Tarim Basin, west China, mainly consisting of lacustrine sediments and associated with fluvial-eolian sands (*24*). Controlled by the plateau uplift and long-term Cenozoic global cooling, the Tarim Basin experienced episodic occurrences of lacustrine environments under warmer climatic conditions during high eccentricity and obliquity and, on the contrary, fluvial-eolian deposits during cooler periods of low eccentricity and obliquity (*24*). The chronostratigraphy was established on the basis of magnetostratigraphic correlation to the CK95 geomagnetic polarity time scale, resulting in a duration of ~7.1 Ma from the Late Miocene to Holocene (*24*). We analyze a high–temporal resolution TOC time series from lacustrine mudstone spanning 5.5 to 7.1 Ma (*24*).

Pliocene to Holocene Lake El'gygytgyn (northeast Russia)

Lake El'gygytgyn is located ~100 km north of the Arctic Circle in northeast Russia (67.5°N, 172°E) and is covered by lake ice for 9 months/year. Scientific drilling in El'gygytgyn crater recovered about 273 m in the 5011-1 composite core (*25*, *26*). A high-precision age model was established on the basis of an $^{40}Ar/^{39}Ar$ age-anchored magnetostratigraphy and correlation to the LR04 marine isotope stack and regional insolation (*25*, *27*). Melles *et al.* (*25*) examined TOC content at 2-cm resolution from the 5011-1 core composite, which permits recognition of all potential orbital signals.

Cycle interpretations

Late Cretaceous Songliao Basin (SK-1s core)

The high-resolution TOC record in the SK-1s core is characterized by consecutive alternating highs and lows of 0.5 to 4% magnitude,

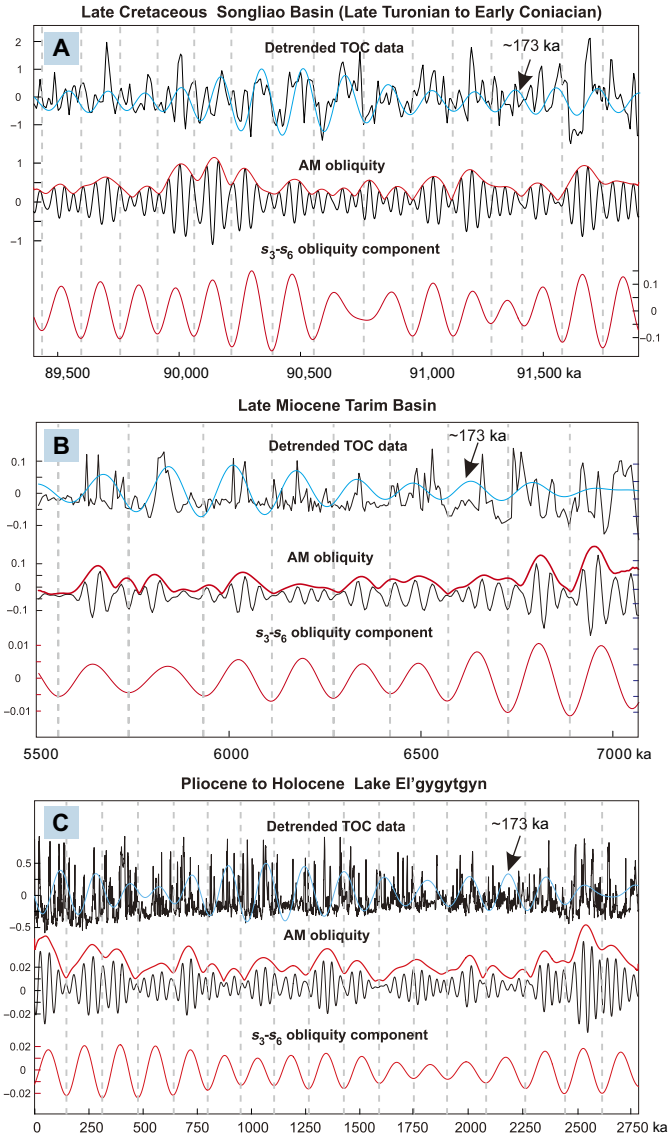

Fig. 2. The obliquity and its ~173-ka amplitude cycle extracted from TOC time series. The detrended TOC data are from (**A**) Songliao Basin, (**B**) Tarim Basin, and (**C**) Lake E1'gygytgyn. The blue lines represent ~173-ka cycles and were extracted from the detrended TOC series with a bandpass of 0.00575 ± 0.001 cycles/ka in these three basins; the obliquity cycles were extracted from the detrended TOC series with a bandpass of 0.0245 ± 0.0085 cycles/ka in (A), 0.026 ± 0.01 cycles/ka in (B), and 0.025 ± 0.007 cycles/ka in (C); Hilbert transform was used to obtain the obliquity AM series. The s_3-s_6 obliquity component was extracted from the orbital obliquity AM curves with a bandpass of 0.00575 ± 0.001 cycles/ka.

superimposed on a long-term decreasing trend (fig. S1). Spectral analysis of the untuned TOC and $\delta^{13}C_{org}$ data from the Qingshankou Formation exhibits cyclicity at wavelengths of 34 to 31, 17 to13.8, 9, 4.5 to 2.5, and 2.3 to 1.77 m (fig. S2). On the basis of the average sedimentation rate (figs. S3 and S4), these cycles represent ~408 to 372, ~204 to 165, ~108, ~57 to 30, and ~27 to 21 ka, respectively (Fig. 3A and fig. S2). The TOC and $\delta^{13}C_{org}$ time series directly adopted the gamma ray (GR) 405-ka tuned age model proposed by Wu *et al.* (*20*).

In addition, to validate the 173-ka cycle interpretation, we also established the floating astronomical time scales (ATSs) by tuning the raw TOC depth series to 405-ka-long eccentricity and to the obliquity AM ~173-ka component, respectively (fig. S5). Power spectral analysis of the two tuned TOC time series shows similar high–confidence level (>90%) peaks around 405, 173, and 60 to 33 ka (figs. S6 and S7). These 60- to 33-ka periods are close to the obliquity band, and the ~173 ka here is ascribed to the obliquity AM cycle s_3-s_6. Notably, the ATSs based on the 173- and 405-ka cycles agree with independent geochronologic data for the core from high-precision U-Pb dating of bentonites (fig. S5) (*21*).

Late Miocene Tarim Basin [Lop Nor (1) borehole]

Liu *et al.* (*24*) published a high-resolution (2- to 4-ka) TOC time series in the 300- to 1050-m depth interval of the Lop Nor (1) core (*24*). The TOC variations at Milankovitch time scales in the core have been attributed to the oscillation between warmer and cooler climates (*24*). Our spectral analysis of the Late Miocene interval of the TOC time series from 5.5 to 7.1 Ma reveals a series of significant cycles (>95%) with periods of 170, 90, 54 to 42, and 23 ka above the 95% confidence level (Fig. 3, C and D).

Pliocene to Holocene El'gygytgyn Lake (ICDP 5011-1)

The high-resolution TOC data from 5011-1 composite core show high-frequency alternations and have been correlated to insolation changes (*25*). Spectral analysis indicates the presence of above 95% significant peaks at 170, 40, 28, 23, and 19 to 14 ka per cycle. In addition, the obliquity AM envelope also shows a series of high-confidence (>99%) signals at 400, 170, and 110 ka per cycle (Fig. 3, E and F).

DISCUSSION

Possible origins of the ~173-ka cycle

In this study, we detect a ~173-ka-period cycle with high confidence (>95%) in a new TOC time series from the Late Cretaceous Songliao Basin (Figs. 2 and 3). In addition, spectral analyses of several other high-resolution TOC series from the Miocene Tarim Basin and Pleistocene Lake El'gygytgyn confirm the presence of a ~173-ka cyclicity in the continental realm from the past 100 Ma (Figs. 2 and 3). Furthermore, our compiled high-resolution records of multiple paleoclimatic proxies in mid-high latitudes throughout the past 200 Ma consistently show enhanced power in the ~160- to 200-ka-period band, which was interpreted to reflect the ~173-ka obliquity AM cycle in the respective original literature (table S1). Recently, a ~200-ka eccentricity cycle was detected in the rhythmically marine sediments from NE Spain and France (*28*). This ~200-ka cycle is generated from alternating strong and weak ~100-ka minima in eccentricity series, most likely originating from the higher fourth- and sixth-order terms in eccentricity and representing nonlinear responses of the climate system to eccentricity components (*29*). However, the similar period of ~173-ka cycle in our TOC series is unlikely to have originated from harmonics of the eccentricity components, due to the weak expression of the basic eccentricity cycle in raw dataset (Figs. 2 and 3 and fig. S2) and due to its presence in obliquity amplitude datasets. The ~173-ka cycle discussed in this study originates from the interaction between obliquity-related frequencies (s_3-s_6) through nonlinear response to obliquity (*14*) or orbital inclination cycles of Earth's elliptical plane. Here, we evaluate and discuss the possible origins of the ~173-ka cycle in TOC series at middle to high latitudes.

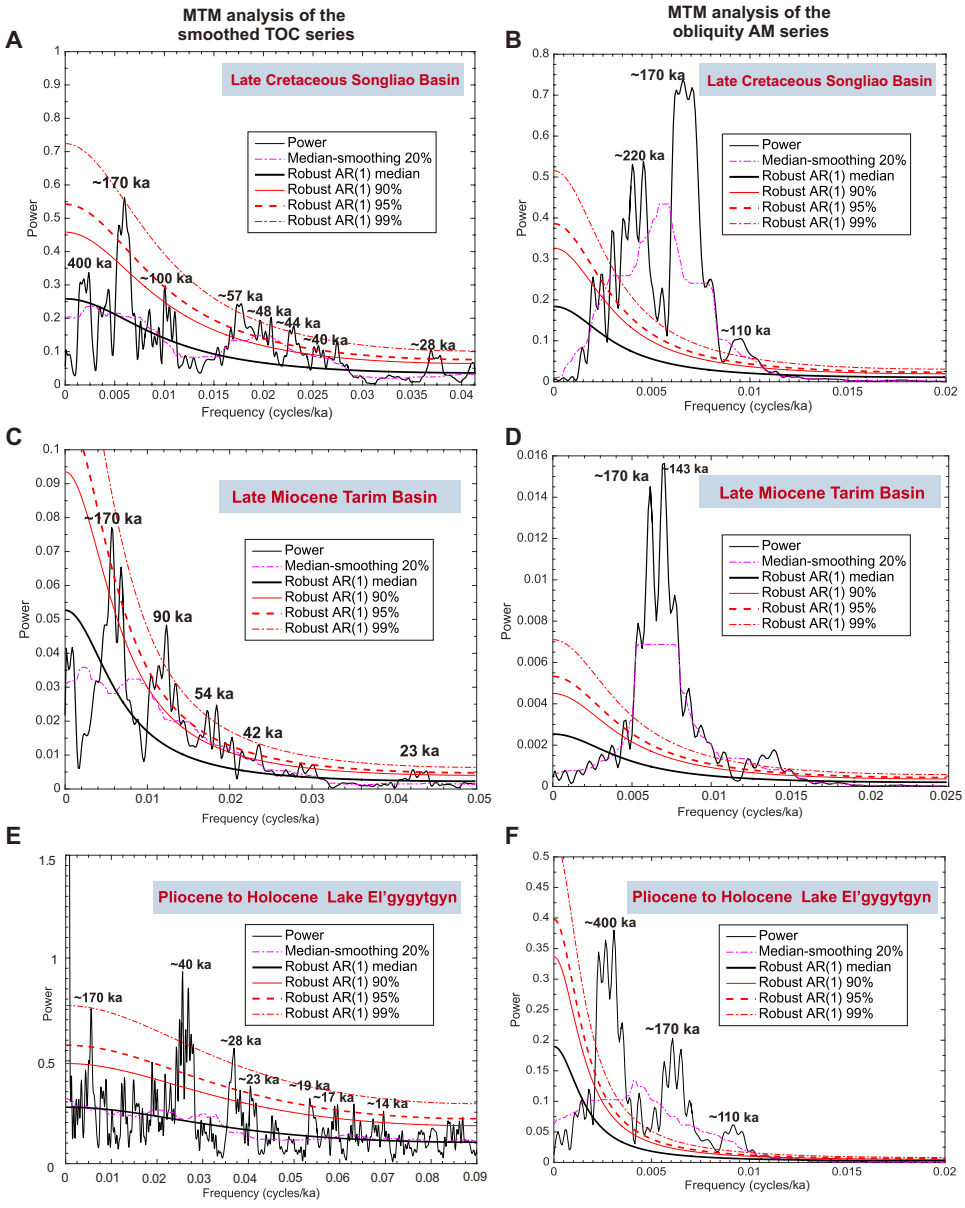

Fig. 3. Spectral analysis of the compiled TOC datasets and their obliquity AM envelopes in the time domain. (**A**) Spectral analysis of the TOC data from Songliao Basin. (**B**) Spectral analysis of the obliquity envelope extracted from the TOC obliquity cycles from Songliao Basin; the age model was based on the tuning GR series to 405-ka-long eccentricity (*20*). (**C**) Spectral analysis of the detrended TOC data from the Tarim Basin. (**D**) Spectral analysis of the obliquity envelope extracted from the TOC obliquity cycles from Tarim Basin. (**E**) 2π MTM analysis of the detrended TOC series from Lake E1′gygytgyn. (**F**) Spectral analysis of the obliquity envelope extracted from the TOC obliquity cycles from Lake E1′gygytgyn.

Earth orbital inclination

Inclination is a fundamental element of the shape and orientation of Earth's orbit and represents the angle between a reference plane and the orbital plane of Earth (*3*). Among the inclination cycles of ~2.4 Ma, ~1.2 Ma, ~173 ka, ~110 ka, and 98 ka (fig. S8), ~173 ka has the lowest signal power. The maximum variation in average total solar insolation from orbital inclination over time scales of thousand years is ~0.003 Wm^{-2}, three orders of magnitude less than for eccentricity (*30*). This minor value suggests that the ~173-ka signal of inclination would barely be detected by paleoclimate proxies and is an insufficient source of the cycle observed in this study.

Obliquity AM

AM analysis is a powerful approach to characterize astronomical forcing patterns (*2*, *3*, *31*, *32*), and indeed, the astronomical solution displays several AMs, which have been detected in the stratigraphic records [e.g., (*5*, *12*–*14*, *33*)]. Earth's obliquity has several long-term modulation cycles due to the individual obliquity frequencies and their interferences, among which two main terms are s_4-s_3 (related to the precession of nodes of Earth and Mars, ~1.2 Ma per cycle) and s_3-s_6 (corresponding to the precession of nodes of Earth and Saturn, ~173 ka per cycle) (*13*, *14*). Both of them depend on the orbital motions of the planets (*1*, *2*, *14*). The s_4-s_3–related ~1.2-Ma

AM phenomenon has been widely detected in stratigraphic records and has been linked to paleoclimate events and eustasy [e.g., (*4*, *11*, *12*, *34*)]. This s_3-s_6 AM cycle has been detected in Late Cretaceous geological archives during OAE2, further extending its usage in constructing floating ATS in pre-Cenozoic records (*13*). We propose the s_3-s_6 AM cycle as the possible origin of the ~173-ka cycle observed in our TOC time series.

Obliquity threshold response model

Clipping is a process that limits an influence to a value range above/below a threshold. Earth's climate is characterized as a dynamic and chaotic system with climatic feedbacks that can clip forcing signals and generate nonlinearities in proxy datasets (*35*, *36*). Here, we calculate the clipped obliquity series based on the La2010d theoretical astronomical solution from 80 to 95 Ma (fig. S8). The clipped obliquity time series shows the same spectral peaks as the original series, but the ~173-ka component is greatly enhanced to an extent of the obliquity amplitude envelope (fig. S8). This amplification mechanism in Earth climate system may be associated with some specific climatic or sedimentary processes within the depositional basins.

OC burial response to obliquity-forced hydrological cycles

Changes in astronomical insolation can influence Earth surface carbon cycle processes (*5*, *15*, *37*, *38*). Obliquity variations mainly influence insolation near the polar circle and modulate high-latitude biomass production via changing the areal extent of polar night regions (*39*). Obliquity also plays the major role in controlling meridional insolation gradients, which affect middle- to high-latitude atmospheric circulation and poleward moisture transport (*40*). These processes can be expected to indirectly pace rainfall, continental weathering rates, riverine fluxes, and lake fertilization (Fig. 4). The TOC records in mid-high latitudes shown here are mainly controlled by the ~40-ka obliquity cycle and a ~173-ka AM of obliquity (Figs. 2 and 3). These cycles may be a signature of quasi-periodic variations in primary productivity and/or preservation conditions of OC, while the main controlling factor for the formation of organic-rich/poor intervals depends on different sedimentary processes.

To interpret the strong ~40- and ~173-ka obliquity signals found in our TOC series, we invoke a model where obliquity-modulated hydrological processes in mid-high latitudes control OC burial (Fig. 4) (*15*). Within the climate system, the carbon cycle is inextricably linked with the hydrological cycle, and climate models predict an enhanced monsoonal wind speed and precipitation between minimum and maximum tilt (*41*). A recent study from the Andaman Sea also confirmed that the obliquity had enhanced the Indian summer monsoon intensity during the latest Miocene warming interval (*42*). These different orbital configurations might also modulate ten thousand– to million-year-scale continental water storage fluctuations (*10*–*12*). A series of recently published astronomically tuned climatic records further demonstrate that obliquity contributes to secular changes in the hydrological cycle, recorded in both lakes and oceans (*4*, *11*, *12*). Therefore, the OC burial cycle, coupled to the hydrologic cycle, could respond to obliquity signals as observed in our integrated TOC data. Hence, high precipitation and weathering rates during the high-obliquity wet season are associated with increased continental runoff and fluvial input (*10*). Moreover, increased nutrient and terrestrial (organic) carbon transfer into sedimentary basins results in productivity blooms, as well as stratified water columns and bottom-water anoxia, reflected in high TOC values. In contrast, low obliquity decreased precipitation and chemical weathering due to less efficient poleward moisture and heat transport, leading to an opposite outcome for OC burial (Fig. 4). These processes can explain the basic ~40-ka obliquity signal in TOC datasets, although the specific mechanism of amplifying the ~173-ka AM cycle is to be explored further.

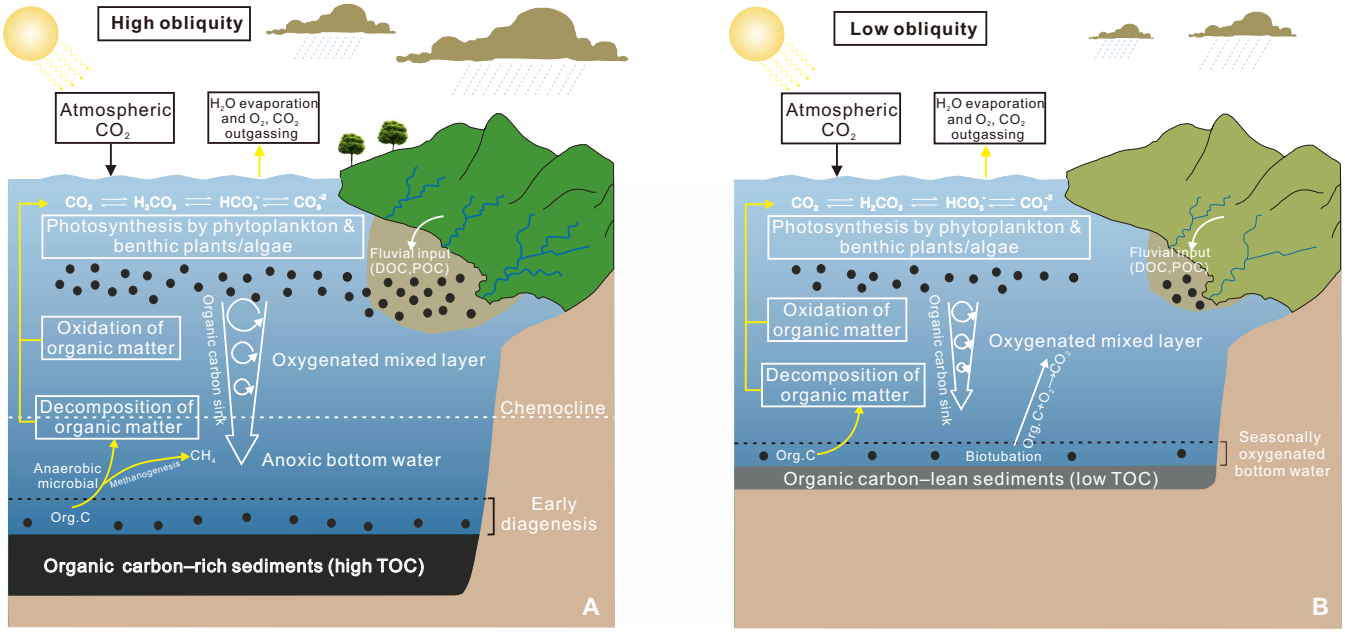

Fig. 4. Obliquity-forced organic carbon burial models. Scheme of lacustrine OC burial linked to maxima (**A**) and minima (**B**) of obliquity. Obliquity maxima are related to summer insolation maxima on both hemispheres. In this model, the OC burial is driven by the local hydrological processes and the basin's geochemical conditions. DOC, dissolved organic carbon; POC, particle organic carbon.

Nonlinear sedimentary processes amplified ~173-ka obliquity AM cycles

It is unexpected that the theoretically low-AM cycles (e.g., ~9 Ma, ~2.4 Ma, ~1.2 Ma, ~400 ka, and ~173 ka in this study) produced significant and identifiable signals in the geological records. These orbital quasi-periodic cycles are considered to have been amplified through nonlinear response feedbacks between external (orbital) forcing and the internal climate and sedimentary systems (*5*, *38*). Earth's climate and sedimentary systems consist of complex feedbacks and feedback chains. Abrupt climate change [e.g., extinction events, OAEs, and Paleocene-Eocene thermal maximum (PETM)], noise, and astronomical signal distortion are three important features in the nonlinear climate system (*7*, *36*). However, what sort of nonlinearities are driven by astronomical forcing is far less clear (*7*). Compared to the shorter Milankovitch cycles (i.e., precession, ~20 ka; obliquity, ~40 ka; and eccentricity, ~100 ka), the longer AM signals (e.g., ~9 Ma, ~2.4 Ma, ~1.2 Ma, and even the ~400-ka-long eccentricity) have been recorded in marine $\delta^{13}C$ series because of the long residence time of carbon in the ocean-atmosphere system, reflecting a nonlinear mechanism associated with memory effects of carbon in the oceans (*5*, *15*, *33*, *38*). The ~1.2-Ma obliquity AM cycle in the $\delta^{13}C_{org}$ record has been suggested as a nonlinear feedback to OC accumulation in Cretaceous strata (*15*). Here, we extend this analogy to the 173-ka cycle and hypothesize that this obliquity AM cycle results from comparable nonlinear forcing of OC burial, thus providing a possible mechanism for the observed cyclicity patterns in TOC records.

According to the spectral results of the three TOC time series, the ~173-ka signal is not only expressed in the obliquity envelope series but also clearly detected in the original TOC datasets (Figs. 2 and 3). This feature indicates that the obliquity AM cycle is not the only contributor for the ~173-ka cycle; there is a specific process to enhance the ~173-ka cycle itself. Here, we provide a possible mechanism related to threshold responses to the obliquity forcing. The ~173-ka AM cycle is enhanced in a scenario of obliquity forcing across a critical geochemical threshold within sedimentary basins (Fig. 5). The equilibrium of the lake biogeochemistry is a considerable "tipping point" capable of clipping the obliquity signal. When the system falls below a threshold, the net OC burial flux is decreased in lacustrine settings owing to oxygenated bottom waters and reduced terrestrial input, resulting in OC-poor sediments (Figs. 4B and 5). Conversely, as obliquity exceeds a critical threshold, the net carbon burial flux is increased through increased carbon export to the bottom and/or enhanced preservation through anoxic bottom conditions (Fig. 5). Therefore, the lake biogeochemical processes can cause a threshold for burial or oxidation of OC [e.g., (*16*)], and thus, this threshold response could transfer the basic high-frequency ~40-ka obliquity cycle to the longer low-frequency AM periods (Fig. 5).

These threshold transitions between distinct states occur in both climate model results and geological records (*43*–*45*). Trigger mechanisms of thresholds are commonly linked in time and can mechanistically be linked to orbital forcing (*36*). Examples of thresholds, due to the high AM of precession and obliquity, also have been observed in the intensification of Neogene glaciations (*46*, *47*) and ocean circulation changes during the PETM (*43*). Moreover, this threshold hypothesis has subsequently been applied to explain the long-term carbon cycle in marine sediments (*15*, *48*).

Terrestrial sedimentary processes recorded in lakes, such as weathering and nutrient delivery, can also affect marginal marine depositional settings, which leads to speculation that our amplified AM threshold model may be useful for explaining the nonlinear interactions between orbital forcing and sedimentary processes in continental margin depositional systems [e.g., East China Sea Shelf Basin (*4*)].

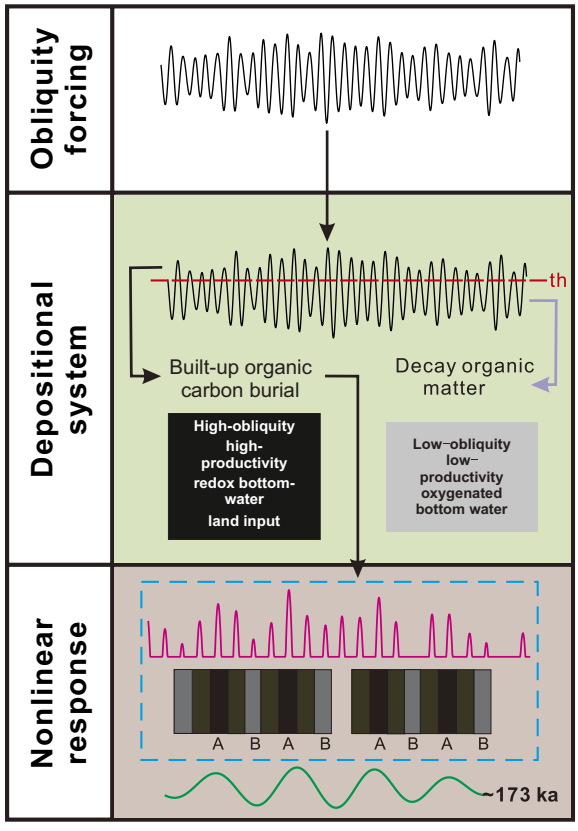

Fig. 5. A simplified possible sedimentary process of nonlinear climate feedback linked to the 173-ka amplitude of obliquity. The external obliquity forcing impact on Earth's surface climate, when exceeding a critical threshold in a depositional system (internal feedback), can leave imprints in the sedimentary sequences. "th" is the abbreviation of "threshold."

The ~173-ka signal recorded in OC isotopes

Theoretically, obliquity-forced OC burial may influence the global carbon cycle, which would ultimately leave imprints on carbon isotope records at all latitudes. We integrate one new high-resolution OC isotope curve from the Songliao Basin (China) with two published curves from the Western Interior Basin (United States) and Bohemian Basin (Czech Republic) in the Cretaceous period to test this hypothesis. All three records exhibit the same obliquity AM signal bands at ~170 ka (Fig. 6) (*15*, *49*, *50*). Although previous studies have documented this cycle, the exact physical processes behind its origin remain unclear (*15*).

The OC burial flux is generally considered the primary lever for driving shifts in $\delta^{13}C$ records, as photosynthetically derived organic matter is isotopically depleted in ^{13}C (i.e., low values of $\delta^{13}C$), and its burial shifts the residual dissolved carbon reservoir to more isotopically enriched values (*51*). The new high-resolution chemostratigraphy from the Songliao Basin preserves the ~170-ka cycle directly in TOC data (Figs. 2 and 3 and fig. S7). In this regard, the

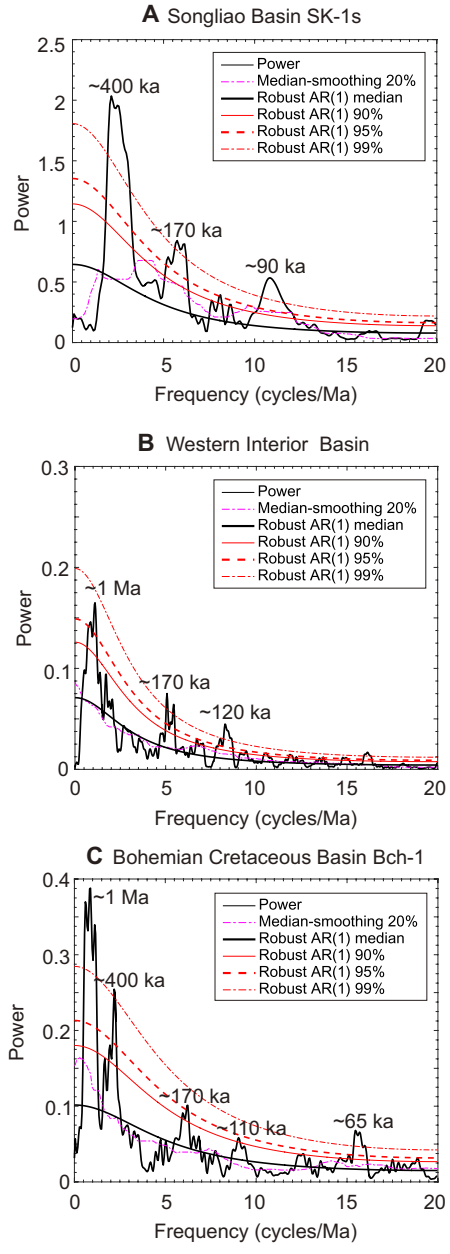

Fig. 6. 2π-MTM power spectral analysis of the compiled Late Cretaceous $\delta^{13}C_{org}$ series. (**A**) Songliao Basin (this study), (**B**) Western Interior Basin (*49*), and (**C**) Bohemian Cretaceous Basin (*50*). A significant ~170-ka cycle is observed in each setting.

occurrence of the ~170-ka cycle in the Cretaceous $\delta^{13}C$ records is consistent with its origin from OC burial in mid-high latitude terrestrial settings. Furthermore, productivity and OC burial in the Songliao Basin and similar lacustrine basins were dominantly driven by runoff of dissolved CO_2 and nutrients (Fig. 4) (*23*). Thus, we infer that the imprint of the ~170-ka obliquity cycle on global-scale $\delta^{13}C$ records in the Cretaceous can be traced, in part, to astronomical forcing of mid-high latitude hydrology and OC burial in the vast paleolakes and expansive wetlands covering continents in the Cretaceous (*52*), as has been postulated for traditional obliquity cycles (*15*).

The geological relevance of the ~173-ka cycle

The discovery of the ~173-ka cycle modulating the global carbon cycle is important from both stratigraphic and paleoclimatic viewpoints. As the 173-ka cycle is derived from the s_3-s_6 term and does not reflect Earth's precession frequency p, its stability extends past 50 Ma (*14*), meaning that the 173-ka cycle has the potential to represent a high-precision astronomical reference curve for orbital tuning. Furthermore, by comparison with the g_2-g_5 (405-ka) term, the 173-ka and 405-ka cycle deviations were nearly the same at the onset of the Late Cretaceous (~100 Ma), indicating that the 173 ka may help as a target cycle to construct floating ATSs back to at least 100 Ma (*13*). Our Late Cretaceous (~90-Ma) TOC series has been tuned to 173 ka and resulted in a reliable floating ATS, which could be comparable with the 405-ka tuning results (figs. S5 and S6). Moreover, the AM hierarchical pattern of obliquity associated with the ~173-ka and ~1.2-Ma cycles may serve as a statistical technique (i.e., "testTilt" in Astrochron R package) to assess the obliquity signal preserved in geological records (*53*). In addition, the detection of these AM cycles (e.g., 173 ka, 1.2 Ma, 2.4 Ma, and ~9 Ma) from the geological archives suggests that the climatic/sedimentary system is sensitive enough to respond to small insolation changes related to obliquity, although they express low-amplitude signals in seasonal insolation data. These AM cycles would have been amplified via nonlinear feedbacks and/or threshold responses and open a new window for deciphering the interactions between orbital forcing and sedimentary processes. This also motivates future work to evaluate specific mechanisms for orbital AM cycle amplification in various depositional systems.

MATERIALS AND METHODS

Construction of the Songliao Basin TOC, C/N, and $\delta^{13}C_{org}$ series

Samples for this study were collected from SK-1s at 1-m resolution from the Qingshankou Formation. A total of 203 samples were collected from member 1 and the bottom of member 2+3. HCL (2N, 1:5 volume) was added to approximately 0.5 g of sample powder and allowed to react for ~24 hours to remove carbonate fraction. The acid was removed, and the sample was brought to a neutral pH through multiple deionized water rinses and dried in an oven. TOC, total nitrogen (TN), and $\delta^{13}C_{org}$ value of the carbonate-free residues were analyzed by Vario EL Cube organic element analyzer and Thermo Fisher Scientific Finnigan Delta V mass spectrometer in the State Key Laboratory of Marine Geology, Tongji University, Shanghai.

The stable isotope composition of the sample is expressed in the standard delta (δ) notation as per mil (‰) deviations from Vienna Pee Dee belemnite. Long-term analytical precision for the stable carbon isotope measurements is 0.1‰ based on replicated analyses (n = 36) on isotope standards (U.S. Geological Survey and acetanilide). For every 10 samples, repeat sample and standard sample were inserted to check the stability and reliability of the instrument.

The C/N value was calculated by TOC and TN values according to the function C/N = (TOC/12.01)/(TN/14.01), where 12.01 is the atomic weight of carbon, and 14.01 is the atomic weight of nitrogen. When calculating the C/N ratio, both TOC and TN are expressed in percentages. We used TN in bulk sediments because in most inorganic sediments, the concentration of inorganic nitrogen is smaller compared to organic nitrogen due to high TOC values.

Spectral analysis of the datasets and astronomical tuning

On the basis of existing age models, our chemostratigraphic sampling resolution in the Qingshankou Formation was conducted at a roughly uniform time interval (~10 ka) from the Songliao Basin (*21*). We also analyzed a compilation of Cretaceous to Quaternary records from previously published TOC and OC isotope datasets from middle to high paleolatitude sedimentary successions (Fig. 1 and table S1). In the following paragraphs, we take the Songliao records as an example to introduce the spectral methods, and other records follow the same spectral procedures.

Cyclicity in sedimentary geochemical proxies was quantified by using the multitaper method (MTM) spectral analyses (*54*) with a red noise null model (*55*) using the Acycle package in MATLAB software (*56*). Key steps before spectral analysis are as follows. First, long-term trends were removed to avoid distortion of low-frequency spectral peaks in the spectrum by using a "Lowess" method to remove weighted average in Acycle software (*56*). Second, the depth series were resampled to obtain evenly spaced data using linear interpolation. The MTM method was applied with three 2π tapers to estimate the spectra of TOC and $\delta^{13}C_{org}$ series in depth domain. The signals of the orbital components were extracted from the data series using a Gaussian bandpass filter in Acycle (*56*). Significance was calculated at 90, 95, and 99% confidence levels for rejecting the null Ar1 model in all spectral analysis processes.

In addition, the average spectral misfit (ASM) method was used to obtain an optimal sedimentation accumulation rate (SAR) for the Qingshankou Formation based on the null hypothesis significance level in Astrochron package in R (*57*). The astronomical frequency targets used in ASM were 1/405 (E), 1/100 (e), 1/50.58 (O1), 1/39.02 (O2), and 1/20.4 (p1) cycles/ka for the Late Cretaceous according to the La2004 model and Berger and Laskar 1992 model (*1*, *58*). Hilbert transform was used to generate the obliquity amplitude envelopes in the Astrochron package in R (*57*).

The 173-ka component cycle extracted from the obliquity amplitude envelopes was subsequently used to establish a floating ATS for Qingshankou Formation in Songliao Basin. By comparing the 173-ka tuning result with the 405-ka tuning result, along with radioisotopic dating of bentonites in the SK-1s core (*21*), we confirmed the accuracy of the 173-ka tuning approach in Late Cretaceous (figs. S5 and S6). Because of the high-precision time scales previously published for the Tarim Basin and Lake El'gygytgyn, we adopted the original age models to the TOC time series and directly conducted spectral analysis on the time-domain TOC series.

Spectral analysis and the ~173-ka floating ATS in Songliao Basin

The MTM power spectrum of the untuned TOC and $\delta^{13}C_{org}$ data through the Qingshankou succession in the Songliao Basin has significant peaks (>90%, *F* test) at wavelengths of 34 to 31, 17 to 13.8, 9, 6.6 to 5.8, 4.5 to 2.8, and 2.5 to 1.77 m (fig.S2). According to the available age model constraints from biostratigraphy, cyclostratigraphy, and U-Pb bentonite ages, 200 plausible evenly spaced sedimentary accumulation rates (SARs) between 6 and 16 cm/ka were tested. Monte Carlo simulation was conducted for each SAR by randomizing the input frequencies for 100,000 trials and ultimately producing an optimal SAR that satisfied the stratigaphic frequencies and the astronomical target frequencies under a minimized misfit value. A null hypothesis significant level (H_0-SL) was given to evaluate the possibility of no astronomical forcing in the sedimentary sequences.

The results of ASM for the Qingshankou Formation indicate an optimal SAR of 8.32 cm/ka with a small H_0-SL of ~0.1% (fig. S3). According to this SAR, the significant peaks in the TOC MTM power spectrum were converted into the temporal domain and result in the cyclicities of 408 ka (34 m), 166 ka (13.8 m), 108 ka (9 m), 79 ka (6.6 m), 54 ka (4.5 m), 40 ka (3.4 m), 30 ka (2.5 m), and 25 ka (2.1 m). Here, the wavelengths of ~34, 9, and 4.5 to 2.5 m are interpreted as the long eccentricity (E), short eccentricity (e), and obliquity (O), respectively.

Late Cretaceous TOC records from the Songliao Basin document a strong obliquity signal with a high-power AM signal. We follow Charbonnier *et al.*'s (*13*) tuning procedure and interpret the wavelength of 13.8- to 17-m cycles in the obliquity AM envelopes as the s_3-s_6 obliquity component in depth domain, and for each cycle, we assigned a 173-ka duration. The TOC record was transformed from depth to time using the bandpass-filtered 173-ka cycle and then linearly interpolated at a uniform grid of 10 ka, which was anchored to a high-precision U-Pb age. We anchored the time scale to the ash bed at a depth of 1705 m with a U-Pb age of 90.974 ± 0.12 Ma, because previous astronomical modeling indicates that this U-Pb age is more suitable (*21*, *23*). To test the accuracy of the 173-ka tuning age, we compared the 173-ka tuning age model with the 405-ka tuning age models based on the raw TOC series, and the two age models showed similar temporal duration and power spectral results, validating our orbital signal interpretation of the 173-ka cycle (figs. S5 and S6).

SUPPLEMENTARY MATERIALS

Supplementary material for this article is available at http://advances.sciencemag.org/cgi/content/full/7/28/eabf9489/DC1

REFERENCES AND NOTES

1. J. Laskar, P. Robutel, F. Joutel, M. Gastineau, A. C. M. Correia, B. Levrard, A long-term numerical solution for the insolation quantities of the Earth. *Astron. Astrophys.* **428**, 261–285 (2004).
2. L. A. Hinnov, New perspectives on orbitally forced stratigraphy. *Annu. Rev. Earth Planet. Sci.* **28**, 419–475 (2000).
3. L. A. Hinnov, Cyclostratigraphy and its revolutionizing applications in the earth and planetary sciences. *Geol. Soc. Am. Bull.* **125**, 1703–1734 (2013).
4. Y. Liu, C. Huang, J. G. Ogg, T. J. Algeo, D. B. Kemp, W. Shen, Oscillations of global sea-level elevation during the Paleogene correspond to 1.2-Myr amplitude modulation of orbital obliquity cycles. *Earth Planet. Sci. Lett.* **522**, 65–78 (2019).
5. M. Martinez, G. Dera, Orbital pacing of carbon fluxes by a approximately ~9-My eccentricity cycle during the Mesozoic. *Proc. Natl. Acad. Sci. U.S.A.* **112**, 12604–12609 (2015).
6. J. A. van Dam, H. A. Aziz, M. Á. Á. Sierra, F. J. Hilgen, L. W. van den Hoek Ostende, L. J. Lourens, P. Mein, A. J. van der Meulen, P. Pelaez-Campomanes, Long-period astronomical forcing of mammal turnover. *Nature* **443**, 687–691 (2006).
7. J. A. Rial, R. A. Pielke Sr., M. Beniston, M. Claussen, J. Canadell, P. Cox, H. Held, N. de Noblet-Ducoudré, R. Prinn, J. F. Reynolds, J. D. Salas, Nonlinearities, feedbacks and critical thresholds within the Earth's climate system. *Clim. Change* **65**, 11–38 (2004).
8. D. C. Nobes, S. F. Bloomer, J. Mienert, F. Westall, Milankovitch cycles and nonlinear response in the quaternary record in the atlantic sector of the Southern Oceans. *Proceedings of the Ocean Drilling Program, Scientific Results* **114**, 551–576 (1991).
9. C. Ma, S. R. Meyers, B. B. Sageman, Theory of chaotic orbital variations confirmed by Cretaceous geological evidence. *Nature* **542**, 468–470 (2017).
10. M. S. Li, C. J. Huang, L. A. Hinnov, J. Ogg, Z. Q. Chen, Y. Zhang, Obliquity-forced climate during the Early Triassic hothouse in China. *Geology* **44**, 623–626 (2016).
11. M. Wang, H. H. Chen, C. J. Huang, D. B. Kemp, T. W. Xu, H. G. Zhang, M. S. Li, Astronomical forcing and sedimentary noise modeling of lake-level changes in the Paleogene Dongpu Depression of North China. *Earth Planet. Sci. Lett.* **535**, 116116 (2020).
12. H. Huang, Y. Gao, M. M. Jones, H. Tao, A. R. Carroll, D. E. Ibarra, H. Wu, C. Wang, Astronomical forcing of Middle Permian terrestrial climate recorded in a large paleolake in northwestern China. *Palaeogeogr. Palaeoclimatol. Palaeoecol.* **550**, 109735 (2020).

13. G. Charbonnier, S. Boulila, J. E. Spangenberg, T. Adatte, K. B. Föllmi, J. Laskar, Obliquity pacing of the hydrological cycle during the Oceanic Anoxic Event 2. *Earth Planet. Sci. Lett.* **499**, 266–277 (2018).
14. S. Boulila, M. Vahlenkamp, D. De Vleeschouwer, J. Laskar, Y. Yamamoto, H. Pälike, S. K. Turner, P. F. Sexton, T. Westerhold, U. Röhl, Towards a robust and consistent middle Eocene astronomical time scale. *Earth Planet. Sci. Lett.* **486**, 94–107 (2018).
15. J. Laurin, S. R. Meyers, D. Uličný, I. Jarvis, B. B. Sageman, Axial obliquity control on the greenhouse carbon budget through middle- to high-latitude reservoirs. *Paleoceanogr. Paleoclimatol.* **30**, 133–149 (2015).
16. M. Ripepe, A. G. Fischer, Stratigraphic rhythms synthesized from orbital variations. *Kansas Geol. Survey Bull.* **233**, 335–344 (1991).
17. M. Ruhl, M. H. L. Deenen, H. A. Abels, N. R. Bonis, W. Krijgsman, W. M. Kürschner, Astronomical constraints on the duration of the early Jurassic Hettangian stage and recovery rates following the end-Triassic mass extinction (St Audrie's Bay/East Quantoxhead, UK). *Earth Planet. Sci. Lett.* **295**, 262–276 (2010).
18. C. Huang, S. P. Hesselbo, L. Hinnov, Astrochronology of the late Jurassic Kimmeridge Clay (Dorset, England) and implications for Earth system processes. *Earth Planet. Sci. Lett.* **289**, 242–255 (2010).
19. X. Wan, J. Zhao, R. W. Scott, P. Wang, Z. Feng, Q. Huang, D. Xi, Late Cretaceous stratigraphy, Songliao Basin, NE China: SK1 cores. *Palaeogeogr. Palaeoclimatol. Palaeoecol.* **385**, 31–43 (2013).
20. H. Wu, S. Zhang, G. Jiang, L. Hinnov, T. Yang, H. Li, X. Wan, C. Wang, Astrochronology of the Early Turonian–Early Campanian terrestrial succession in the Songliao Basin, northeastern China and its implication for long-period behavior of the solar system. *Palaeogeogr. Palaeoclimatol. Palaeoecol.* **385**, 55–70 (2013).
21. T. Wang, J. Ramezani, C. Wang, H. Wu, H. He, S. A. Bowring, High-precision U–Pb geochronologic constraints on the Late Cretaceous terrestrial cyclostratigraphy and geomagnetic polarity from the Songliao Basin, Northeast China. *Earth Planet. Sci. Lett.* **446**, 37–44 (2016).
22. C. L. Deng, H. Y. He, Y. X. Pan, R. X. Zhu, Chronology of the terrestrial Upper Cretaceous in the Songliao Basin, Northeast Asia. *Palaeogeogr. Palaeoclimatol. Palaeoecol.* **385**, 44–54 (2013).
23. M. M. Jones, D. E. Ibarra, Y. Gao, B. B. Sageman, D. Selby, P. Chamberlain, S. A. Graham, Evaluating Late Cretaceous OAEs and the influence of marine incursions on organic carbon burial in an expansive East Asian paleo-lake. *Earth Planet. Sci. Lett.* **484**, 41–52 (2018).
24. W. Liu, Z. Liu, Z. An, J. Sun, H. Chang, N. Wang, J. Dong, H. Wang, Late Miocene episodic lakes in the arid Tarim Basin, western China. *Proc. Natl. Acad. Sci. U.S.A.* **111**, 16292–16296 (2014).
25. M. Melles, J. Brigham-Grette, P. S. Minyuk, N. R. Nowaczyk, V. Wennrich, R. M. De Conto, P. M. Anderson, A. A. Andreev, A. Coletti, T. L. Cook, E. Haltia-Hovi, M. Kukkonen, A. V. Lozhkin, P. Rosén, P. Tarasov, H. Vogel, B. Wagner, 2.8 million years of Arctic climate change from Lake El'gygytgyn, NE Russia. *Science* **337**, 315–320 (2012).
26. J. Brigham-Grette, M. Melles, P. Minyuk, A. Andreev, P. Tarasov, R. De Conto, S. Koenig, N. Nowaczyk, V. Wennrich, P. Rosén, E. Haltia, T. Cook, C. Gebhardt, C. Meyer-Jacob, J. Snyder, U. Herzschuh, Pliocene warmth, polar amplification, and stepped pleistocene cooling recorded in NE Arctic Russia. *Science* **340**, 1421–1427 (2013).
27. P. W. Layer, Argon-40argon-39 age of the El'gygytgyn impact event, Chukotka, Russia. *Meteorit. Planet. Sci.* **35**, 591–599 (2000).
28. F. Hilgen, C. Zeeden, J. Laskar, Paleoclimate records reveal elusive ~200-kyr eccentricity cycle for the first time. *Global Planet. Change* **194**, 103296 (2020).
29. F. J. Hilgen, H. A. Abels, K. F. Kuiper, L. J. Lourens, M. Wolthers, Towards a stable astronomical time scale for the Paleocene: Aligning Shatsky Rise with the Zumaia – Walvis Ridge ODP site 1262 composite. *Newsl. Stratigr.* **48**, 91–110 (2015).
30. L. E. A. Vieira, A. Norton, T. D. de Wit, M. Kretzschmar, G. A. Schmidt, M. C. M. Cheung, How the inclination of Earth's orbit affects incoming solar irradiance. *Geophys. Res. Lett.* **39**, L16104 (2012).
31. C. Zeeden, S. R. Meyers, L. J. Lourens, F. J. Hilgen, Testing astronomically tuned age models. *Paleoceanogr. Paleoclimatol.* **30**, 369–383 (2015).
32. S. R. Meyers, The evaluation of eccentricity related amplitude modulation and bundling in paleoclimate data: An inverse approach for astrochronologic testing and time scale optimization. *Paleoceanogr. Paleoclimatol.* **30**, 1625–1640 (2015).
33. S. Boulila, B. Galbrun, J. Laskar, H. Pälike, A ~9myr cycle in Cenozoic $\delta^{13}C$ record and long-term orbital eccentricity modulation: Is there a link? *Earth Planet. Sci. Lett.* **317-318**, 273–281 (2012).
34. M. Li, L. A. Hinnov, C. Huang, J. G. Ogg, Sedimentary noise and sea levels linked to land-ocean water exchange and obliquity forcing. *Nat. Commun.* **9**, 1004 (2018).
35. J. A. Rial, Abrupt climate change: Chaos and order at orbital and millennial scales. *Global Planet. Change* **41**, 95–109 (2004).
36. R. B. Alley, J. Marotzke, W. D. Nordhaus, J. T. Overpeck, D. M. Peteet, R. A. Pielke Jr., R. T. Pierrehumbert, P. B. Rhines, T. F. Stocker, L. D. Talley, J. M. Wallace, Abrupt climate change. *Science* **299**, 2005–2010 (2003).
37. S. R. Meyers, B. B. Sageman, M. A. Arthur, Obliquity forcing of organic matter accumulation during Oceanic Anoxic Event 2. *Paleoceanogr. Paleoclimatol.* **27**, PA3212 (2012).
38. M. S. Storm, S. P. Hesselbo, H. C. Jenkyns, M. Ruhl, C. V. Ullmann, W. Xu, M. J. Leng, J. B. Riding, O. Gorbanenko, Orbital pacing and secular evolution of the Early Jurassic carbon cycle. *Proc. Natl. Acad. Sci. U.S.A.* **117**, 3974–3982 (2020).
39. P. Huybers, Early Pleistocene glacial cycles and the integrated summer insolation forcing. *Science* **313**, 508–511 (2006).
40. M. E. Raymo, K. H. Nisancioglu, The 41 kyr world: Milankovitch's other unsolved mystery. *Paleoceanogr. Paleoclimatol.* **18**, 1011 (2003).
41. J. H. C. Bosmans, F. J. Hilgen, E. Tuenter, L. J. Lourens, Obliquity forcing of low-latitude climate. *Clim. Past* **11**, 1335–1346 (2015).
42. J. Jöhnck, W. Kuhnt, A. Holbourn, N. Andersen, Variability of the Indian monsoon in the Andaman Sea across the Miocene-Pliocene transition. *Paleoceanogr. Paleoclimatol.* **35**, PA003923 (2020).
43. J. P. Kennett, L. D. Stott, Abrupt deep-sea warming, palaeoceanographic changes, and benthic extinctions at the end of the Palaeocene. *Nature* **353**, 225–229 (1991).
44. W. D. Sellers, A global climatic model based on the energy balance of the earth-atmosphere system. *J. Appl. Meteorol. Climatol.* **8**, 392–400 (1969).
45. H. Stommel, Thermohahe convection with two stable regimes of flow. *Tellus* **2**, 224–230 (1961).
46. L. J. Lourens, J. Becker, R. Bintanja, F. J. Hilgen, E. Tuenter, R. S. W. van de Wal, M. Ziegler, Linear and nonlinear response of Late Neogene glacial cycles to obliquity forcing and implications for the Milankovitch theory. *Quat. Sci. Rev.* **29**, 352–365 (2010).
47. J. Imbrie, J. Z. Imbrie, Modeling the climatic response to orbital variations. *Science* **207**, 943–953 (1980).
48. B. S. Cramer, J. D. Wright, D. V. Kent, M.-P. Aubry, Orbital climate forcing of $\delta^{13}C$ excursions in the Late Paleocene-Early Eocene (chrons C24n-C25n). *Paleoceanogr. Paleoclimatol.* **18**, 1097 (2003).
49. Y. J. Joo, B. B. Sageman, Cenomanian to Campanian carbon isotope chemostratigraphy from the Western Interior Basin, U.S.A. *J. Sediment. Res.* **84**, 529–542 (2014).
50. D. Uličný, I. Jarvis, D. R. Gröcke, S. Čech, J. Laurin, K. Olde, J. Trabucho-Alexandre, L. Švábenická, N. Pedentchouk, A high-resolution carbon-isotope record of the Turonian stage correlated to a siliciclastic basin fill: Implications for mid-Cretaceous sea-level change. *Palaeogeogr. Palaeoclimatol. Palaeoecol.* **405**, 42–58 (2014).
51. L. R. Kump, M. A. Arthur, Interpreting carbon-isotope excursions: Carbonates and organic matter. *Chem. Geol.* **161**, 181–198 (1999).
52. W. W. Hay, R. M. DeConto, P. de Boer, S. Flögel, Y. Song, A. Stepashko, Possible solutions to several enigmas of Cretaceous climate. *Int. J. Earth Sci.* **108**, 587–620 (2019).
53. C. Zeeden, S. R. Meyers, F. J. Hilgen, L. J. Lourens, J. Laskar, Time scale evaluation and the quantification of obliquity forcing. *Quat. Sci. Rev.* **209**, 100–113 (2019).
54. D. J. Thomson, Spectrum estimation and harmonic analysis. *Proc. IEEE* **70**, 1055–1096 (1982).
55. M. E. Mann, J. M. Lee, Robust estimation of background noise and signal de-tection in climatic time series. *Clim. Change* **33**, 409–445 (1996).
56. M. S. Li, L. A. Hinnov, L. Kump, *Acycle*: Time-series analysis software for paleoclimate research and education. *Comput. Geosci.* **127**, 12–22 (2019).
57. S. R. Meyers, Astrochron: an R package for astrochronology (2014); http://cran.r-project.org/package=astrochron.
58. A. Berger, M. F. Loutre, J. Laskar, Stability of the astronomical frequencies over the Earth's history for Paleoclimate studies. *Science* **255**, 560–566 (1992).
59. S. Kim, B.-K. Khim, K. Takahashi, Late Pliocene to early pleistocene (2.4-1.25 Ma) paleoproductivity changes in the Bering sea: IODP expedition 323 hole U1343E. *Deep Sea Res. Part II Top. Stud. Oceanogr.* **125-126**, 155–162 (2016).
60. C. Huang, L. Hinnov, Astronomically forced climate evolution in a saline lake record of the Middle Eocene to Oligocene, Jianghan Basin, China. *Earth Planet. Sci. Lett.* **528**, 115846 (2019).
61. G. Charbonnier, S. Boulila, S. Gardin, S. Duchamp-Alphonse, T. Adatte, J. E. Spangenberg, K. B. Föllmi, C. Colin, B. Galbrun, Astronomical calibration of the Valanginian "Weissert" episode: The Orpierre marl–limestone succession (Vocontian Basin, southeastern France). *Cretac. Res.* **45**, 25–42 (2013).
62. S. Boulila, B. Galbrun, L. A. Hinnov, P.-Y. Collin, J. G. Ogg, D. Fortwengler, D. Marachand, Milankovitch and sub-Milankovitch forcing of the Oxfordian (Late Jurassic) Terres Noires Formation (SE France) and global implications. *Basin Res.* **22**, 717–732 (2010).
63. S. Boulila, B. Galbrun, E. Huret, L. A. Hinnov, I. Rouget, S. Gardin, A. Bartolini, Astronomical calibration of the Toarcian Stage: Implications for sequence stratigraphy and duration of the early Toarcian OAE. *Earth Planet. Sci. Lett.* **386**, 98–111 (2014).
64. K. M. Cohen, S. C. Finney, P. L. Gibbard, J. X. Fan, The ICS International Chronostratigraphic Chart. *Episodes* **36**, 199–204 (2018).
65. S. R. Meyers, Cyclostratigraphy and the problem of astrochronologic testing. *Earth Sci. Rev.* **190**, 190–223 (2019).

66. B. Galbrun, S. Boulila, L. Krystyn, S. Richoz, S. Gardin, A. Bartolini, M. Maslo, "Short" or "long" Rhaetian? Astronomical calibration of Austrian key sections. *Global Planet. Change* **192**, 103253 (2020).
67. Y. Zhong, H. Wu, J. Fan, Q. Fang, M. Shi, S. Zhang, T. Yang, H. Li, L. Cao, Late Ordovician obliquity-forced glacio-eustasy recorded in the Yangtze Block, South China. *Palaeogeogr. Palaeoclimatol. Palaeoecol.* **540**, 109520 (2020).

Acknowledgments: We thank L. Niu and T. Dong for help with preparing figures and table and X. M. Cao, Y. Y. Duan, and X. Tian for assistance with sampling. We deeply thank L. D. Chen and Z. F. Liu for accessing the analytical facilities at Tongji University. We thank editor Dr. Cin-Ty Lee and two reviewers for helpful and constructive comments. **Funding:** This study was supported by the National Natural Science Foundation of China (grant nos. 41888101, 41790450, and 41972096), the National Key R&D Plan (2019YFC0605405), the China Geological Survey project (DD20190010), Key Scientific and Technological Project of RIPED (2021ycq01), and the "111" project (B20011). D.E.I. is supported by the UC Berkeley Miller Institute for Basic Research and UC President's Postdoctoral Fellowships. **Author contributions:** H.H., Y.G., and C.W. designed the research; H.H. and Y.G. compiled the datasets and analyzed the data. H.H. prepared the figures and table. H.H. and Y.G. wrote the manuscript with contributions from C.M., M.M.J., C.Z., D.E.I., H.W., and C.W. All authors revised the manuscript. **Competing interests:** The authors declare that they have no competing interests. **Data and materials availability:** All data needed to evaluate the conclusions in the paper are present in the paper and/or the Supplementary Materials. Additional data related to this paper may be requested from the authors.

Submitted 1 December 2020
Accepted 26 May 2021
Published 9 July 2021
10.1126/sciadv.abf9489

Citation: H. Huang, Y. Gao, C. Ma, M. M. Jones, C. Zeeden, D. E. Ibarra, H. Wu, C. Wang, Organic carbon burial is paced by a ~173-ka obliquity cycle in the middle to high latitudes. *Sci. Adv.* **7**, eabf9489 (2021).